Am J Cancer Res 2023;13(5):1923-1937
www.ajcr.us /ISSN:2156-6976/ajcr0146776

Original Article

Plasma-derived exosomal immunoglobulins IGHV4-4 and IGLV1-40 as new non-small cell lung cancer biomarkers

Peng Yang[1], Yang Zhang[1], Ruping Zhang[1], Yun Wang[1], Shengjin Zhu[1], Xin Peng[1], Yimin Zeng[1], Bing Yang[1], Meijun Pan[1], Jie Gong[2], Hongping Ba[2]

[1]*The Second Affiliated Hospital, Guizhou University of Traditional Chinese Medicine, Guiyang, Guizhou, PR China;* [2]*Department of Clinical Laboratory, Wuhan Center for Clinical Laboratory, Wuhan, Hubei, PR China*

Received September 29, 2022; Accepted April 7, 2023; Epub May 15, 2023; Published May 30, 2023

Abstract: Exosomal proteins represent valuable research directions in the liquid biopsy of lung cancer (LC). Immunoglobulin subtypes, immunoglobulin molecules with different domains in variable regions, are products of B cell responses to different tumor antigens and are associated with tumor incidence and development. The plasma of patients with LC should theoretically contain a large number of B cell-derived exosomes that specifically recognize tumor antigens. This paper intended to assess the value of the proteomic screening of plasma exosomal immunoglobulin subtypes for diagnosing non-small cell LC (NSCLC). The plasma exosomes of NSCLC patients and healthy control participants (HCs) were isolated using ultracentrifugation. Label-free proteomics was employed to assess the differentially expressed proteins (DEPs), while the biological characteristics of the DEPs were analyzed using GO enrichment. The immunoglobulin content in the top two fold change (FC) values of the DEPs and the immunoglobulin with the lowest *P*-value were verified using an enzyme-linked immunosorbent assay (ELISA). The differentially expressed immunoglobulin subtypes verified via ELISA were selected to statistically analyze the receiver operating characteristic curve (ROC), after which the diagnostic values of the NSCLC immunoglobulin subtypes were determined via the ROC area under the curve (AUC). The plasma exosomes of the NSCLC patients contained 38 DEPs, of which 23 were immunoglobulin subtypes, accounting for 60.53%. The DEPs were mainly related to the binding between immune complexes and antigens. The ELISA results showed significant differences between the immunoglobulin heavy variable 4-4 (IGHV4-4) and immunoglobulin lambda variable 1-40 (IGLV1-40) in the LC patients and HCs. Compared with the HCs, the AUCs of IGHV4-4, IGLV1-40, and a combination of the two in diagnosing NSCLC were 0.83, 0.88, and 0.93, respectively, while the AUCs for non-metastatic cancer were 0.80, 0.85, and 0.89. Moreover, their diagnostic values for metastatic cancer compared to non-metastatic cancer displayed AUCs of 0.71, 0.74, and 0.83, respectively. When IGHV4-4 and IGLV1-40 were combined with serum CEA to diagnose LC, the AUC value increased, exhibiting values of 0.95, 0.89, and 0.91 for the NSCLC, non-metastatic, and metastatic groups, respectively. Plasma-derived exosomal immunoglobulins containing IGHV4-4 and IGLV 1-40 domains can provide new biomarkers for diagnosing NSCLC and metastatic patients.

Keywords: Exosome, diagnostic biomarkers, non-small-cell lung cancer, immunoglobulin heavy variable 4-4, immunoglobulin lambda variable 1-40

Introduction

As the leading histological lung cancer (LC), non-small cell lung cancer (NSCLC) accounts for about 85% of all LC incidences [1] and produces malignant tumors with the fastest increase in morbidity and mortality. Early diagnosis and treatment are vital for reducing the LC mortality rate and improving recovery. Early detection of LC can reportedly reduce the mortality rate 10-50-fold, and patients can even recover after early surgery [2]. The current methods for diagnosing LC include lung tissue biopsies, imaging examination, and classic serum markers, such as CEA. However, these tests are either invasive or nonspecific, and their diagnostic level does not meet the requirements of LC treatment [3]. Consequently, establishing more sensitive, specific, and non-invasive methods is crucial for diagnosing the

occurrence and metastasis of LC and improving the overall survival rate.

Exosome liquid biopsy is the most valuable research approach in examining early tumor diagnostic markers. Exosomes are small vesicles encapsulated by lipid bilayer-secreted cells, with diameters of about 30-150 nm, containing molecules with original cell information, such as tumor cell- and B cell-mediated tumor immunity, including proteins, RNA molecules, and lipids, displaying significant potential for early tumor recognition [4]. Under the protection of the exosomal lipid bilayer membrane, these protein information molecules can avoid protease hydrolysis, substantially increasing their lifespan [5, 6]. Compared with liquid biopsy, such as circulating free DNA (*cfDNA*) and circulating *tumor* cells (*CTCs*), exosomal proteins labeled tumor have more advantages, for exsample, the concentration of exosomal proteins is higher and easier to be detected [7, 8]. However, existing studies on exosomal tumor protein markers focus on the protein information molecules derived from tumor cells, while little is known about the exosomal immunoglobulin derived from B cells that mediate tumor immunity.

The variable immunoglobulin region is highly diverse and vital in human health. The high subtypes and different variable domain of immunoglobulins in serum give individuals with a great potential to recognize various antigens [9, 10]. Some immunoglobulin subtypes, such as immunoglobulin heavy variable (IGHV) and immunoglobulin lambda variable (IGLV) genes, are related to clinical outcomes. For example, the unfavorable prognosis of follicular lymphoma patients [11] is affiliated with the presence of IGHV5, while autoantigens [12] and commensal bacteria [13] are both related to systemic lupus erythematosus (SLE) [14] and bound by IGHV4-34. Theoretically, during the early stage of LC, B lymphocytes that mediate tumor immunity release exosomes into the blood, containing immunoglobulin subtypes that specifically recognize early tumor antigens. This study screens the differentially expressed immunoglobulin in the NSCLC plasma exosomes using proteomic technology and verifies whether their subtypes displaying prominent differential expression can be utilized as markers for NSCLC diagnosis using an enzyme-linked immunosorbent assay (ELISA). Further examination evaluates their NSCLC and metastatic diagnostic value using receiver operating characteristic (ROC) curves to provide a clinical basis for developing exosomal immunoglobulin markers for liquid NSCLC biopsy.

Methods and materials

Patients and clinical samples

A total of 121 NSCLC patients (76 males and 45 females; mean age, 61.4 years; range 54 to 73) were enrolled in this study at the Second Affiliated Hospital of Guizhou University of Traditional Chinese Medicine (Guiyang, China) from January 2018 to December 2020. All patients were pathologically confirmed as having NSCLC. None of the patients had received antitumor treatment before, while those meeting the following criteria were excluded from this study: 1) preoperative chemotherapy or radiotherapy; 2) previous or coexistent tuberculosis or malignant disease. According to the tumor and metastasis classification system [15], 51 of these were metastatic patients, and 70 were non-metastatic. Healthy individuals (76 males and 45 females; mean age, 46.5 years; range 40 to 51) were recruited from outpatients, and a general medical examination showed no immune diseases or tumors. This study used nine non-metastatic patients and nine healthy individuals for proteomics research, while 28 patients and 28 healthy individuals were used to validate the target protein of the screening. The remaining 84 patients and 84 healthy individuals were used for ROC analysis. After admission, blood was collected from the patients. The blood was centrifuged for 30 min at 2000 g and 10 min at 1800 g (4°C) to remove cells and cell debris. Next, the supernatant was stored at -80°C for downstream analyses [16, 17]. This study used pathologically confirmed patients who had not undergone chemotherapy or radiotherapy within the previous two months. This research was authorized by the Ethics Committee of the Second Affiliated Hospital of Guizhou University of Traditional Chinese Medicine (KYW-2019002). All participants signed a written consent form for using their blood samples for medical research before the examination.

Isolating the exosomes

Ultracentrifugation was employed to isolate the exosomes in the plasma samples using a proto-

col adapted from that described by Théry et al. [18]. All procedures were performed at 4°C unless otherwise specified. Briefly, the plasma samples were defrosted on ice, after which they were centrifugated for 30 min at 2,000 g and 45 min at 12,000 g to eliminate larger vesicles. Next, a 0.22-μm pore filter was used for supernatant filtration, after which it was ultracentrifuged for 120 min at 110,000 g. After discarding the supernatant and resuspending the exosome pellets in 10 ml 1× phosphate-buffered saline (PBS), they were ultracentrifuged again for 70 min at 110,000 g. The supernatant was discarded, followed by exosome pellet resuspension in either 1× PBS or ice-cold lysis buffer (Beyotime Biotechnology, Shanghai, China) with a protease inhibitor cocktail (ABclonal, Wuhan, China) for further experiments.

Determining the protein concentration

A BCA protein assay kit (Boster Biological Technology, Wuhan, China) was used according to the instructions of the manufacturer to determine the exosomal protein concentration. The total proteins of the exosomes were estimated using a multifunctional enzyme-labeling instrument (Varioskan LUX, Thermo Fisher Scientific, USA).

Exosomal nanoparticle tracking assessment

The exosome pellets were examined using a nano gold system (Izon Science Ltd., Christchurch, New Zealand) according to the instructions of the manufacturer to determine the sizes and quantities of the isolated particles.

Transmission electron microscopy (TEM)

The isolated exosomes (10 μL) were added dropwise to a 100-mesh formvar-coated copper grid for 1 min while the floating liquid was absorbed using filter paper. Uranyl acetate (10 μL) was then added to the copper net to facilitate precipitation for 1 min, using filter paper for floating liquid absorption. The TEM images were obtained at 80 kV after the samples were dried for 5 min to 10 min at room temperature.

Western blot

Here, 12% sodium dodecyl sulfate (SDS)-polyacrylamide gel was used to separate 20 μg protein extract, after which a semi-dry transfer system was employed for relocation to a PVDF membrane. Next, 5% evaporated skimmed milk containing TBS-Tween 20 (0.05%) was used for blocking at room temperature for 2 h, followed by overnight, 4°C membrane incubation with the primary antibodies against CD9 (ab92726, Abcam, Cambridge, UK) and TSG-101 (ab125011, Abcam, Cambridge, UK). Next, the membranes were incubated for 2 h with HRP-coupled secondary antibodies (Feiyi Biotech, Wuhan, China). Photographic film and ECL blotting detection reagents were employed for protein band visualization (Thermo, Waltham, MA, USA).

Proteomic assessment

Preparing the samples: The plasma exosomes of nine patients were divided into three random groups. Each group contained a mixture of plasma exosomes from three patients labeled LC1-3, LC4-6, and LC7-9. Similarly, the plasma exosomes of the nine healthy individuals were selected and randomly divided into three groups labeled HC1-3, HC4-6, and HC7-9. The exosomes were isolated as described above.

SDS-PAGE analysis: Here, 12% Sodium dodecyl sulfate-polyacrylamide gel electrophoresis (SDS-PAGE) was used to separate a 100-μg aliquot of extracted proteins, which was stained with Coomassie G to investigate the changes in the exosomal protein expression. Then, 1 mm^3 cubes were prepared using the minced gel fractions, which were reduced with a 5 mmol/L dithiothreitol (DTT) solution, incubated for 1 h at 37°C, and rehydrated overnight in a 10 ng/μL trypsin solution at 37°C [19]. A 20-μL 1:1 mixture of 0.1% trifluoroacetic acid (TFA) and H_2O/acetonitrile was used to extract the digested peptides from the gel pieces for 15 min. Next, the mixture was subjected to spinning, after which the supernatant was harvested, followed by another extraction for 15 min using a 20-μL 1:2 mixture of 0.1% TFA and H_2O/acetonitrile. The accumulated supernatants were dried in a SpeedVac for LC-MS/MS analysis [20].

LC-MS/MS analysis: The freeze-dried powder was dissolved in 10 μL of the mobile phase (100% water and 0.1% formic acid), followed by 4°C centrifugation for 20 min at 14,000 g, after which a 1 μg sample of the supernatant

was inserted into a C18 column. Linear gradient elution was used to separate the peptides, which were analyzed using a Q Exactive HF-X mass spectrometer (Thermo, Waltham, MA, USA) equipped with a Nanospray Flex™ ion source (ESI) at a 2.4 kV spray voltage, a 275°C transport capillary temperature, an m/z 350 to m/z 1500 full scan range and 120000 resolution (at m/z 200), a 3×10^6 automatic gain control (AGC) target value, and an 80 ms maximum ion injection time. The 40 precursors denoting the highest abundance during the full scan were fragmented via higher-energy collisional dissociation (HCD) and assessed using MS/MS at 15000 resolution (at m/z 200), a 5×10^4 AGC target value, a 45 ms maximum ion injection time, and 27% normalized collision energy. The term ".raw" signified the raw MS detection data.

Data analysis: The Proteome Discoverer 2.4 software was used to analyze the raw MS data, which were compared against the *Homo sapiens* database in the Universal Protein Resource Knowledge Base (UniProt KB). The initial search exhibited a 15-ppm precursor mass window, following the trypsin enzymatic cleavage rule, which allowed a maximum of 20 ppm mass tolerance and two missed cleavage sites for the fragment ions. Methionine oxidation, N-terminal acetylation, and methionine oxidation were regarded as variable alterations, while cysteine carbamidomethylation was deemed a fixed modification during the database search. During the protein identification and peptide-spectrum match (PSM), the global false discovery rate (FDR) limit was P<0.01. Only proteins that were consistently recognized by at least two separate peptides in a minimum of two sample replicates were considered present and investigated further.

Data processing and protein quantification: The label-free quantification (LFQ) of each discovered protein was calculated according to the peptide signal intensities. The MaxLFQ algorithm in MaxQuant was used to measure the protein abundance of the identified peptides. The experimental samples were subjected to match-between-runs to obtain the quantified information of all replicates. Perseus provided default distribution parameters for the low-abundance proteins displaying missing values. A two-way Student's t-test was used to analyze the statistical significance and quantify the proteins. Proteins displaying a P<0.05 significance value and a >1.5 fold change (FC) when comparing the two groups were designated differentially expressed proteins (DEPs), while log2 (FC) was used for further analysis.

ELISA

The ELISA kits for IGHV4-4, IGLV1-40, and IGLV3D-20 were personalized by EIAab Science Co. Ltd. (Wuhan, China). ELISA kits were used according to the protocol prescribed by the manufacturer to determine the IGHV4-4, IGLV1-40, and IGLV3D-20 concentrations.

Serum CEA measurements

The CEA level was tested using an electrochemiluminescence immunoassay, as well as CEA kits and a Roche Cobas E602 immunology analyzer (Roche Diagnostics, Germany).

Statistical analysis

The differences between the two groups were assessed using Mann-Whitney tests, indicating statistical significance at P<0.05. The predictive value of the tested biomarkers to discriminate between the patients and the HC group or between non-metastatic and metastatic patients was determined using the area under the curve (AUC) for specificity and sensitivity. A student's t-test and one-way or two-way analysis of variance followed by Tukey's posthoc test was used to compare the data of two or multiple groups using the GraphPad Prism V9 software (San Diego, CA, USA). *P*-values below 0.05 were considered statistically significant.

Results

Isolating the plasma exosomes in the clinical samples

The flow chart of this study is shown in **Figure 1**. The exosomes in the plasma samples of the HC and NSCLC patients were isolated via UC, as shown in **Figure 2A**. The exosomes were identified using TEM, nanoparticle tracking analysis (NTA), and WB. TEM indicated typical cup-shaped vesicles (**Figure 2B**), while NTA showed that these vesicles were approximately 80 nm in diameter, with a primary peak size of

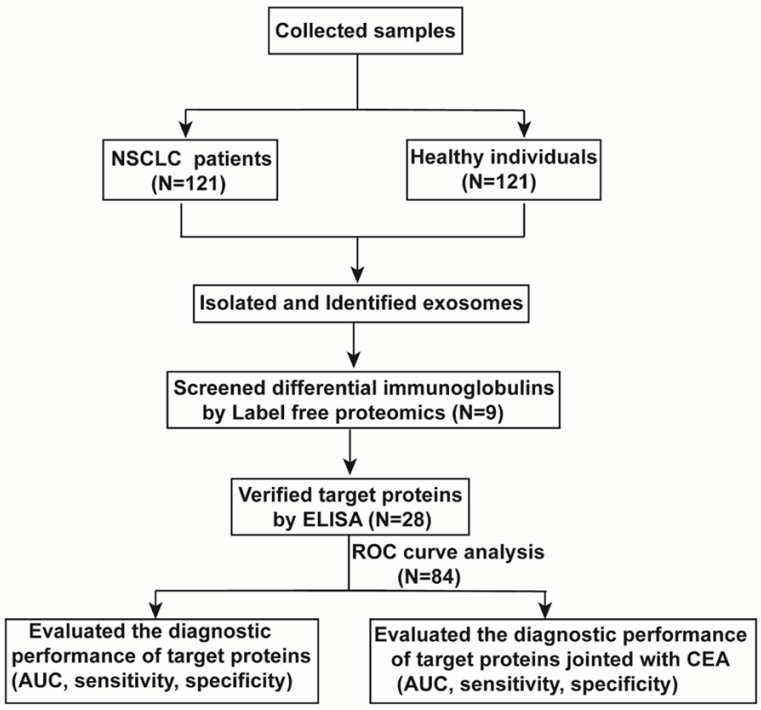

Figure 1. The flow chart of this study. The exosomes from the NSCLC patients and HCs were obtained step-by-step according to the flow chart.

110 nm (**Figure 2C**). Moreover, a BCA protein assay kit was used to determine the plasma exosome protein level. The results indicated no significant differences between the total exosomal protein concentrations of the HC participants and NSCLC patients (**Figure 2D**). The WB results indicated significant TSG 101 and CD 9 exosomal marker expression in the exosomal samples (**Figure 2E**). These findings demonstrated that the exosomes were successfully isolated in the plasma samples of the NSCLC and HC participants.

Proteomic analysis of the plasma exosomes

The six identified exosomal proteins were analyzed via principal component analysis (PCA) to assess the reliability of the data for subsequent analysis. The results showed that the top two PCs accounted for 64.4% of the data variance, while the HC participants and NSCLC patients were clustered into two distinct groups (**Figure 3A**), suggesting a pronounced PCA effect. The label-free proteomic analysis detected 249 individual exosomal plasma proteins. Of these, 238 and 246 proteins were detected in the NSCLC and HC groups, respectively (**Figure 3B**). A quantitative ratio of more than 1.5 was considered upregulation, while a ratio below 0.667 was considered downregulation. Compared with the HCs, the NSCLC groups induced 38 DEPs, 32 of which were upregulated and six downregulated, as shown in the DEP clustering heat map (**Figure 3C**). The top 15 differentially expressed immunoglobulin subgroups of the exosomes of the NSCLC patients and HCs are shown in **Table 1**.

GO enrichment assessment of the DEPs

The 38 DEPs were subjected to GO pathway enrichment analysis using bioinformatics tools to understand their functional significance. This assessment was divided into three primary sections: biological processes (BP), molecular functions (MF), and cellular components (CC). It showed that a large number of DEPs in the CC section were mainly enriched in the term with immunoglobulin complexes (**Figure 4A** and **4B**; Supplementary Table 1), while immunoglobulin receptor binding and antigen binding represented the most abundant terms of DEPs in the MF section (**Figure 4C** and **4D**; Supplementary Table 2). Consequently, these DEPs may be related to tumor immune response.

The IGLV1-40 and IGHV4-4 immunoglobulin subgroups can serve as diagnostic markers for NSCLC

As shown in **Figure 5A**, besides the HC and NSCLC comparison ($P<0.05$), no significant differences were evident between the total exosomal protein content of the other groups. Therefore, the proteins displaying significant FC value changes, such as IGHV4-4 and IGLV1-40, were investigated. The expression levels of the IGHV4-4 and IGLV1-40 plasma exosomes were verified in 56 samples via ELISA. Moreover, the immunoglobulin subtype (IGLV3d-20) displaying the most significant *P*-value change was selected as the control. The detection results for antibody specificity are shown in **Figure 5B**. The anti-IGHV4-4, IGLV1-40, and

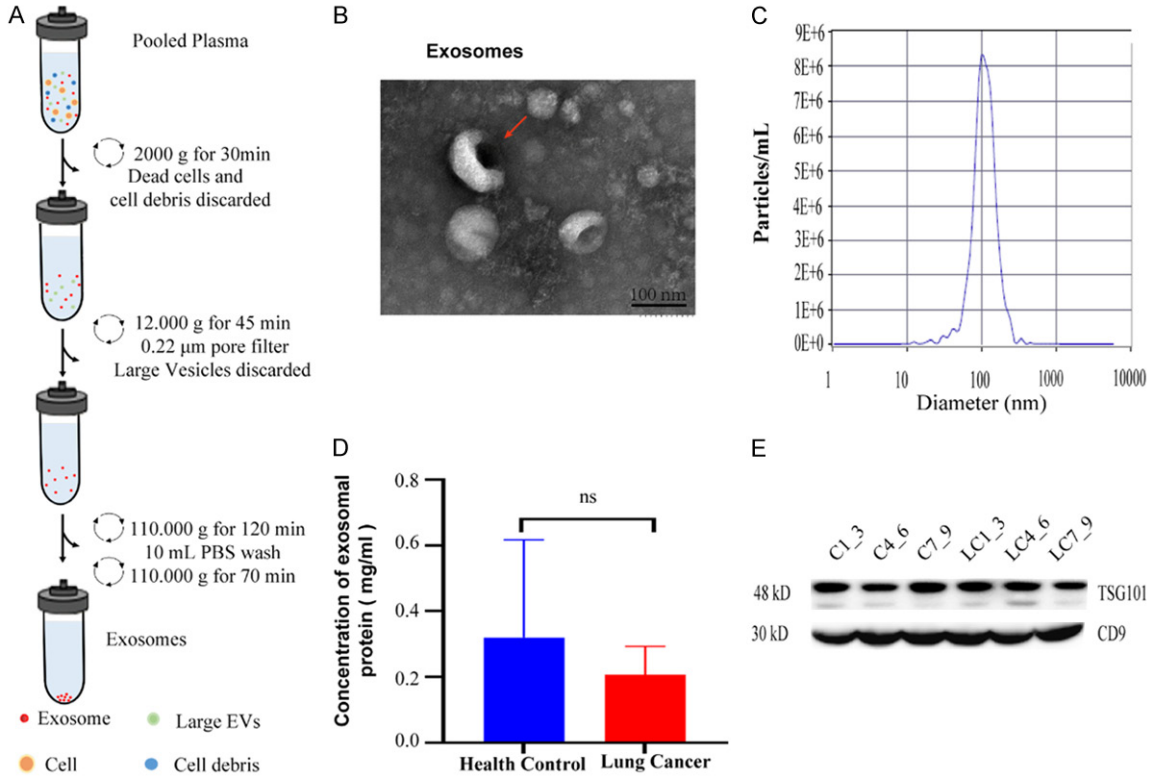

Figure 2. Isolation and characterization of the plasma exosomes. A. A flow chart showing the plasma exosome separation via ultracentrifugation. B. The TEM images of the plasma exosomes. Scale bar =100 nm. The red arrows refer to the exosomes with characteristic cup shapes. C. The plasma exosomal size distribution obtained via NTA. D. The quantitative results of the total proteins of the NSCLC patients and HCs (n=3, each group). ns: not significant. E. The WB analysis of the CD9 and TSG101 exosome markers, using plasma without exosomes as a control.

IGLV3d-20 antibodies only recognized their respective antigenic peptides and did not cross-react with other antigenic peptides. This demonstrated that the antibodies from these kits were only suitable for specifically recognizing their respective immunoglobulin subtypes, preventing a rise in the nonspecific detection level caused by a cross-reaction. The IGLV1-40 test results are shown in **Figure 5C**, indicating significantly elevated exosomal IGLV1-40 levels in the plasma of the NSCLC ($P<0.0001$) and non-metastatic groups, compared with the HCs ($P<0.0001$), as well as the non-metastatic group compared with the metastatic patients ($P<0.01$). Similarly, significant differences were apparent between the IGHV4-4 levels of the NSCLC ($P<0.0001$) or non-metastatic patients ($P<0.001$) and HCs, as well as between the metastatic and non-metastatic patients ($P<0.01$) (**Figure 5D**). However, no substantial differences were evident between the exosomal IGLV3d-20 levels of the NSCLC or non-metastatic patients and the HCs, or between the metastatic and non-metastatic patients (**Figure 5E**). The results confirmed that IGLV1-40 and IGHV4-4 immunoglobulin displayed potential for NSCLC diagnosis.

Furthermore, the relationships between the exosomal IGLV1-40 or IGHV4-4 expression and clinicopathological NSCLC parameters were also analyzed. The IGLV1-40 and IGHV4-4 levels were considerably lower in the metastatic than the non-metastatic patients (**Table 2**).

ROC analysis of the biomarkers

The diagnostic ability of the IGHV4-4 and IGLV1-40 exosomal protein biomarkers was determined by calculating the AUC. A comparison between the NSCLC patients and HCs indicated that the IGHV4-4 proteins displayed a 0.83 AUC (95% CI, 0.75-0.91) with a sensitivity of 85.92% and specificity of 70.00% (**Figure 6A**), while IGHV1-40 presented a 0.88 AUC (95% CI, 0.81-0.96) with a sensitivity of 90.14% and specificity of 80.00% (**Figure 6B**). Moreover, combining the two proteins showed better diag-

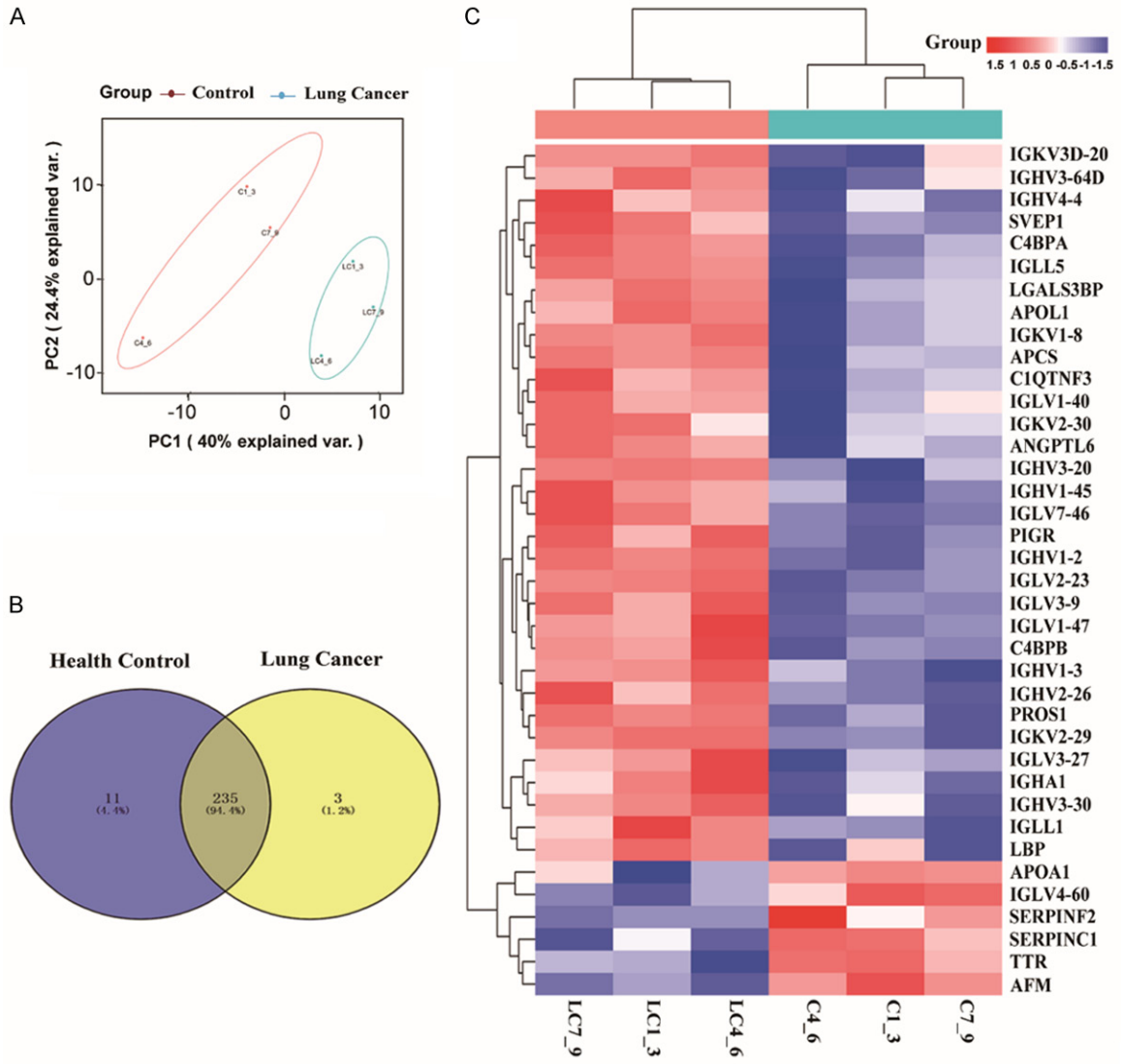

Figure 3. The proteomic assessment of the plasma exosomes in the NSCLC and HC samples. A. The PCA of the plasma exosomes in the NSCLC and HC samples. B. A Venn diagram showing the exosomal protein dispersion. C. A clustering heat map of 38 proteins identified via the t-test. The high and low expression levels of each protein are depicted in red and green.

nostic capacity, with a 0.93 AUC (95% [CI], 0.88-0.97), a sensitivity of 88.73%, and a specificity of 85.00% (**Figure 6C**). The two proteins also displayed excellent diagnostic values for non-metastatic patients and HCs, with AUC values of 0.80 and 0.85, a sensitivity of 83.71% and 86.67%, and a specificity of 70.33% and 80.14% specificity, respectively (**Figure 6D** and **6E**). In addition, the AUC value for combined diagnosis was 0.89, with 86.05% sensitivity and 81.03% specificity (**Figure 6F**). Moreover, the diagnostic ability of these two biomarkers in metastatic patients was also analyzed. Compared with non-metastatic patients, IGHV4-4 and IGLV1-40 showed AUCs of 0.71 (95% CI, 0.57-0.84) and 0.74 (95% CI, 0.62-0.87), with 46.22% and 76.87% sensitivity and 93.31% and 73.13% specificity, respectively (**Figure 6G** and **6H**). Combining the two biomarkers produced an AUC of 0.83 (95% CI, 0.74-0.93) with a sensitivity of 83.34% and specificity of 77.81% (**Figure 6I**).

Combining exosomal immunoglobulins and CEA markers improves the capacity to diagnose NSCLC in patients

Combining IGHV4-4 and CEA for NSCLC diagnosis produced a 0.87 AUC (95% CI, 0.81-0.94) with a sensitivity of 81.67% and specificity

Table 1. The top 15 differentially expressed immunoglobulins subgroups between the exosomes of NSCLC patients and HCs

Uniprot accession	Gene symbol	Protein name	FC	P
P01703	IGLV1-40	Immunoglobulin lambda variable 1-40	6.676299	0.010556
A0A075B6R2	IGHV4-4	Immunoglobulin heavy variable 4-4	4.654506	0.000379
P23083	IGHV1-2	Immunoglobulin heavy variable 1-2	3.900602	0.01815
A0A0J9YX35	IGHV3-64D	Immunoglobulin heavy variable 3-64D	3.790055	0.000229
P01705	IGLV2-23	Immunoglobulin lambda variable 2-23	3.655951	0.01823
P01700	IGLV1-47	Immunoglobulin lambda variable 1-47	3.606699	0.021486
A0A075B6I9	IGLV7-46	Immunoglobulin lambda variable 7-46	2.762598	0.016114
A0A0A0MS14	IGHV1-45	Immunoglobulin heavy variable 1-45	2.607885	0.015263
A2NJV5	IGKV2-29	Immunoglobulin kappa variable 2-29	2.506589	0.033438
A0A0B4J1V2	IGHV2-26	Immunoglobulin heavy variable 2-26	2.463827	0.027487
A0A0C4DH25	IGKV3D-20	Immunoglobulin kappa variable 3D-20	2.43075	0.000181
A0A0C4DH32	IGHV3-20	Immunoglobulin heavy variable 3-20	2.428193	0.015222
P06310	IGKV2-30	Immunoglobulin kappa variable 2-30	2.413879	0.013255
A0A0C4DH67	IGKV1-8	Immunoglobulin kappa variable 1-8	2.290831	0.004608
A0A0C4DH29	IGHV1-3	Immunoglobulin heavy variable 1-3	2.192177	0.026449

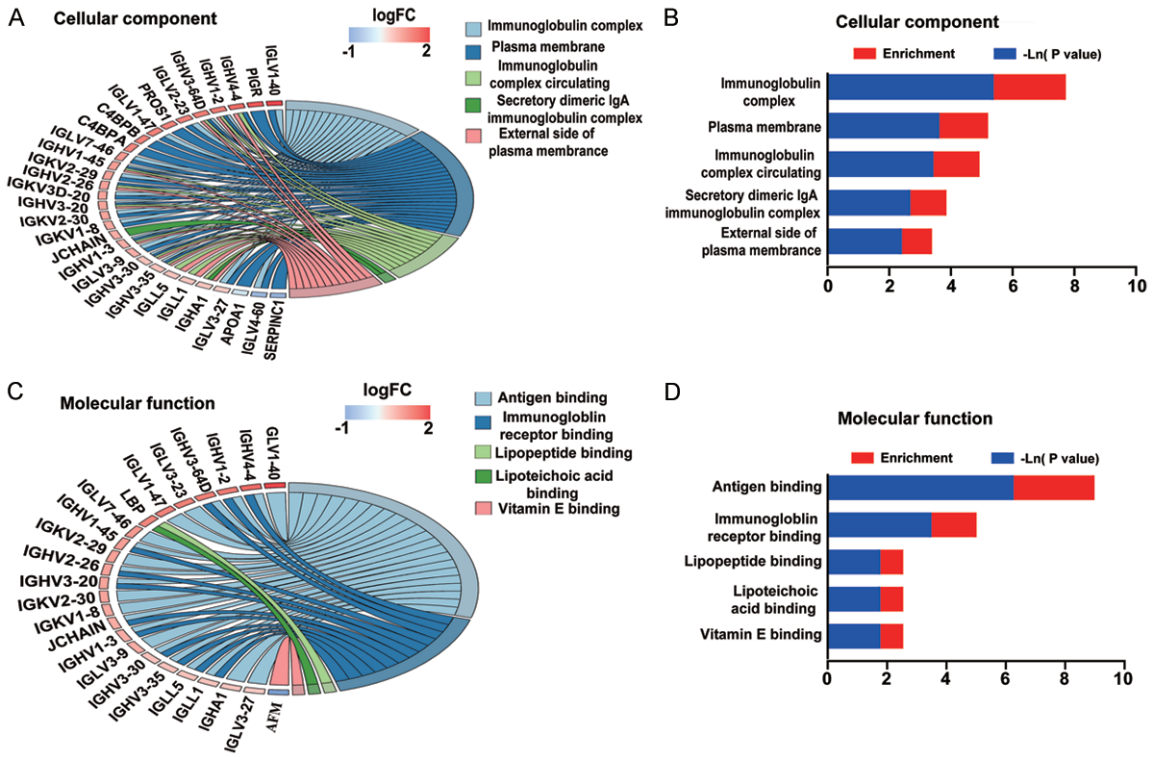

Figure 4. The GO analysis chord plots of the DEPs. The top five enriched terms of the DEP CCs (A) and the top five enriched terms of the DEP MFs (C). Chord plots are circular dendrograms showing expression profile clustering. The *p*-value and enrichment in CC (B) and MF (D). The blue abscissa represents the *p*-value, while the red represents the enrichment. Log FC: log2 (fold changes); -Ln (*P*-value): -log10 (*P*-value).

of 77.50%, exceeding that of CEA alone (AUC=0.78, with a sensitivity of 70.00% and specificity of 76.67%) (**Figure 7A**). Consequently, combining IGLV1-40 and CEA significantly improved the diagnostic efficiency (AUC=0.92, 95% CI, 0.86-0.97), with optimal specificity and sensitivity of 85.00% and 90.00%, respectively (**Figure 7B**). The diagnostic capacity

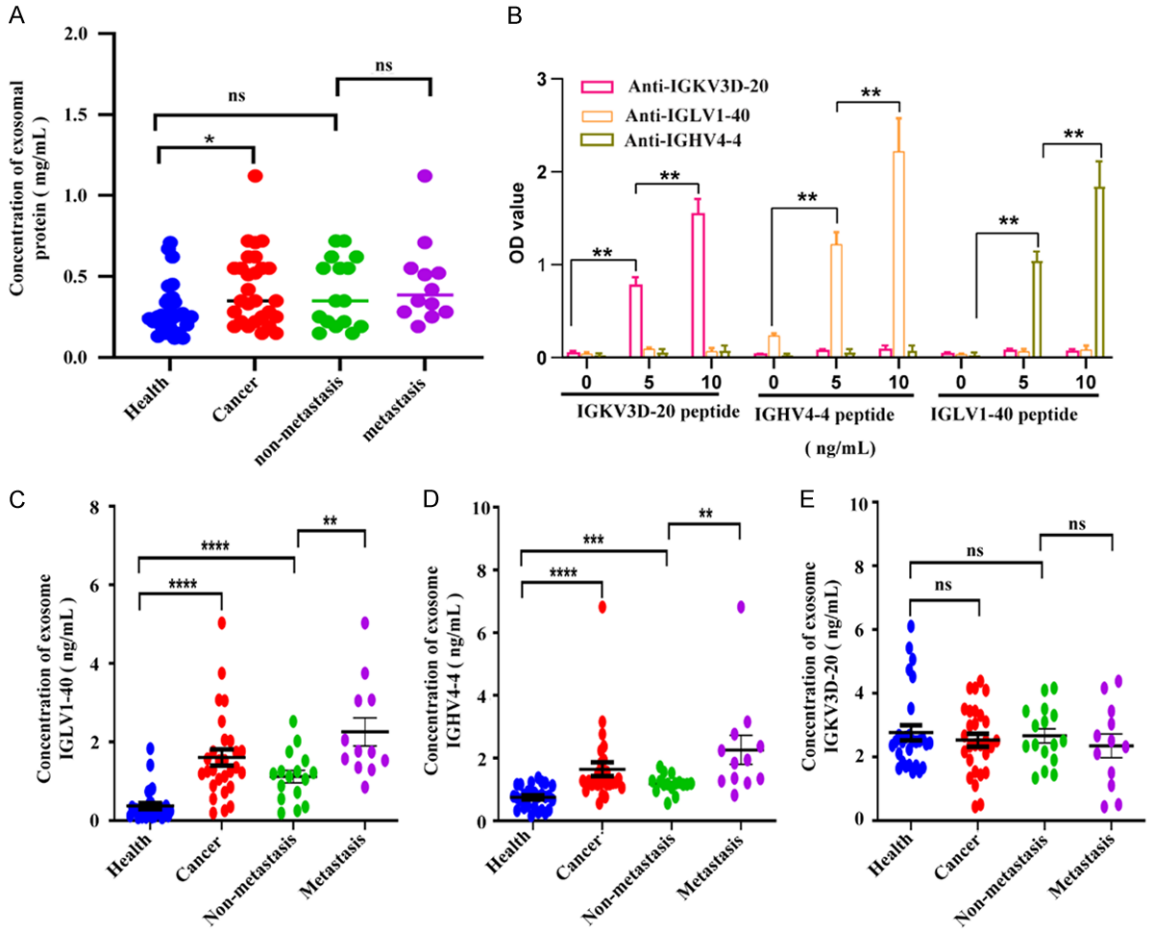

Figure 5. Verification of the plasma exosomal IGHV4-4, IGLV3d-20, and IGLV1-40 protein expression levels in the NSCLC patients. The Mann-Whitney U-test was employed to compare the group expression levels. ns: not significant. *P<0.05, **P<0.01, ***P<0.0001, and ****P<0.00001. A. The quantitative results of the total proteins in the different groups. B. The specificity of the three different antigenic peptides identified via the anti-IGHV4-4, IGLV3d-20, and IGLV1-40 antibodies, respectively. C. The exosomal IGLV1-40 concentration in the HC (n=28), NSCLC (n=28), non-metastatic (n=16), and metastatic groups (n=12). D. The exosomal IGHV4-4 concentration in the different groups. E. The exosomal IGLV3D-20 concentration in the different groups.

increased when IGHV4-4 and IGLV1-40 were combined with CEA (AUC=0.95, 95% CI, 0.90-0.99), displaying 90.00% sensitivity and 85.00% specificity (**Figure 7C**; Supplementary Table 3).

Similarly, the combined diagnostic ability of these new markers significantly exceeded that of CEA alone in non-metastatic patients compared with HCs. The AUC of IGHV4-4 or IGLV1-40 combined with CEA was 0.84 (95% CI, 0.75-0.93) with a sensitivity of 78.95% and specificity of 82.50% (**Figure 7D**) and 0.86 (95% CI, 0.77-0.94) with a sensitivity of 73.68% and specificity of 85.00% (**Figure 7E**), respectively. The AUC of IGHV4-4 and IGLV1-40 combined with CEA was 0.89 (95% CI, 0.82-0.96), with a sensitivity of 76.32% and specificity of 82.50% (**Figure 7F**).

Moreover, combining these markers can also effectively differentiate between metastatic and non-metastatic patients. The AUC value of IGHV4-4 was 0.83 (95% CI, 0.72-0.95) when combined with CEA, with a sensitivity of 72.73% and specificity of 86.84% (**Figure 7G**), while the IGLV1-40 displayed a 0.87 AUC (95% CI, 0.79-0.96) when combined with CEA, with 54.55% sensitivity and 92.11% specificity (**Figure 7H**). IGHV4-4 and IGLV1-40 combined with CEA showed a higher diagnostic ability, exhibiting a 0.91 AUC (95% CI, 0.83-0.98), a sensitivity of 72.73%, and specificity of 89.47% (**Figure 7I**; Supplementary Table 4).

Table 2. Relationship between exosomal IGLV1-40 or IGHV4-4 expression and clinicopathological parameters in NSCLC

Characteristics	No. cases	IGLV1-40		IGHV4-4	
		Median (ng/mL)	*P*-value	Median (ng/mL)	*P*-value
Age (year)					
<60	18	1.537	0.271	1.211	0.158
≥60	53	1.281		1.534	
Sex					
Male	51	1.355	0.989	1.531	0.204
Female	20	1.358		1.251	
Smoking status					
Smoker	38	1.366	0.913	1.372	0.415
Non-smoker	33	1.344		1.344	
Histological type					
Adenocarcinoma	57	1.374	0.577	1.336	0.407
Squamous cell	14	1.231		1.212	
Metastasis					
Positive	45	1.073	0.002**	1.239	0.004**
Negative	26	1.817		1.822	

**represents a comparison between metastatic cancer and lung metastatic cancer, P<0.01.

Discussion

Exosome liquid biopsy focuses on diagnostic tumor markers [21-25]. The current research involving NSCLC plasma exosomes primarily concentrates on microRNA. Minimal studies are available regarding exosome proteins, especially B-cell-derived exosome immunoglobulin, that mediate tumor immunity. In this study, the proteomic analysis indicated that the plasma exosomes of patients with NSCLC displayed various differentially expressed immunoglobulin subtypes, compared with the HCs, which may be ideal biomarkers for NSCLC diagnosis.

Immunoglobulin subtypes are encoded by immunoglobulin variable region gene fragments to determine the specific immunoglobulin antigen recognition domain, playing a vital role in tumor immunity, antiviral activity, autoimmune diseases, and inflammation [22, 26-30]. Disease susceptibility is related to germline immunoglobulin heavy-chain (IGHV) gene variation [31]. Compared with ethnically matched healthy individuals, systemic lupus erythematosus (SLE) patients with nephritis exhibit a 2.8-fold homozygous GHV3-30*01 and IGHV3-30-3 deletion enrichment. Furthermore, SLE patients exhibiting these deletions displayed higher anti-DNA antibody titers [32, 33]. This deletion is associated with susceptibility to chronic idiopathic thrombocytopenic purpura [34] and Kawasaki disease [35]. Multiple sclerosis (MS) susceptibility is associated with the positive effect of B-cell depletion therapy and IGHV2 gene polymorphism [36, 37]. Furthermore, IGHV gene mutation is closely linked to the efficacy and prognosis of chronic lymphocytic leukemia [38, 39]. However, the current research involving immunoglobulin subtypes mostly focuses on gene detection and less on the protein identification of immunoglobulin subtypes. This study selected two immunoglobulin subtypes displaying the most significant FC value changes and one immunoglobulin subtype exhibiting the lowest *P*-value for ELISA identification. The ELISA results showed no significant differences between the IGLV3d-20 NSCLC and HC groups. However, the IGLV1-40 and IGHV4-4 levels differed significantly between the NSCLC and HC groups, the non-metastatic and HC groups, and the metastatic and non-metastatic groups. Since immunoglobulin subtypes may display similar structures, the antibodies against one subtype may bind to other subtype molecules to cause cross-reactions. This study identified the antibody specificity of the three different immunoglobulin subtypes. The results indicated the antibodies specifically recognized only the corresponding immunoglobulin subtypes, confirming that using ELISA de-

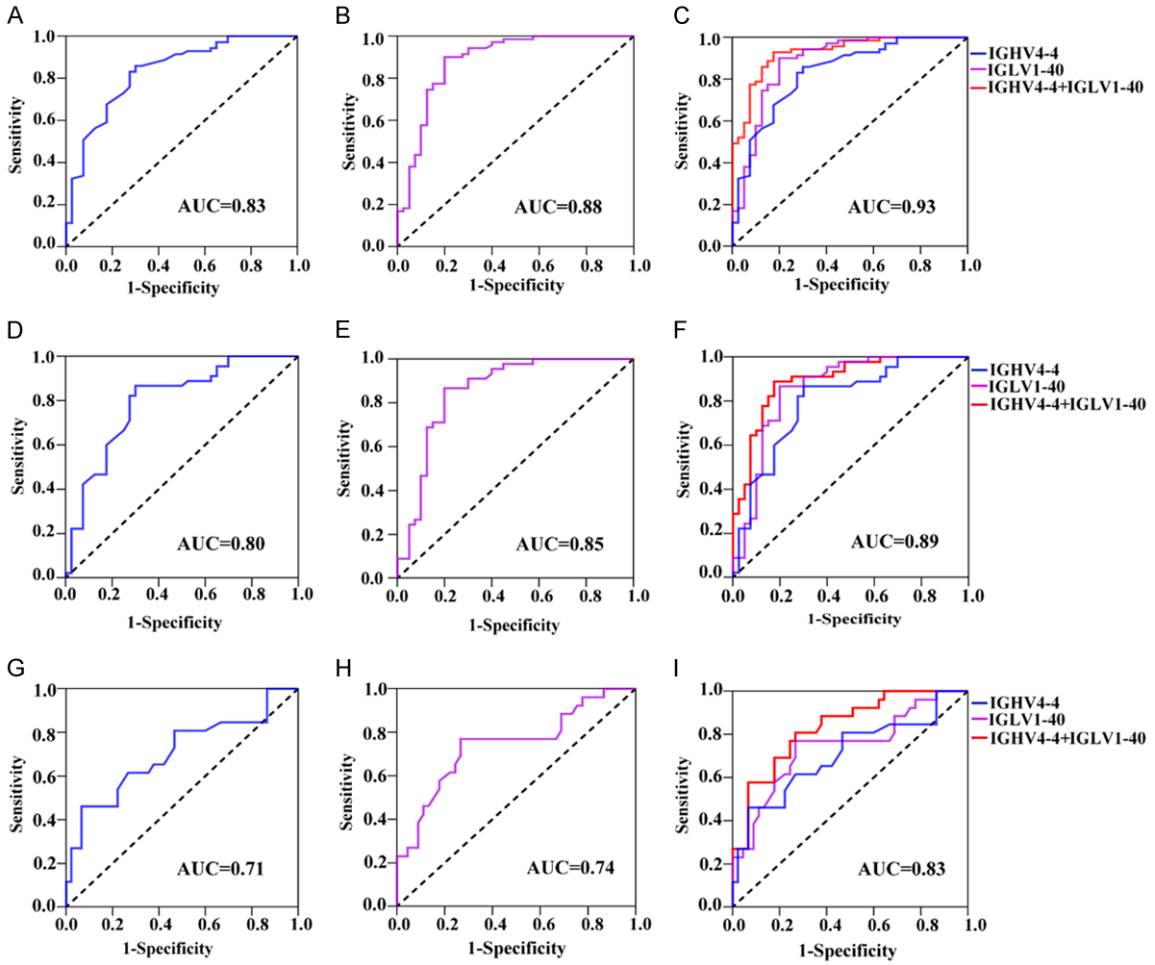

Figure 6. The ROC curve analysis of the exosomal IGLV1-40 and IGHV4-4 for NSCLC diagnosis. (A-C) The ROC curves to distinguish between the NSCLC patients (n=84) and the HCs (n=84). The ROC curves of IGHV4-4 (A), IGLV1-40 (B), and a combination of IGHV4-4 and IGLV 1-40 (C). (D-F) The ROC curves to distinguish between the non-metastatic patients (n=45) and the HCs. The ROC curves of IGHV4-4 (D), IGLV1-40 (E), and a combination of IGHV4-4 and IGLV1-40 (F). (G-I) The ROC curves to distinguish between the metastatic (n=39) and non-metastatic groups. The ROC curves of IGHV4-4 (G), IGLV1-40 (H), and a combination of IGHV4-4 and IGLV1-40 (I).

tection for immunoglobulin subtypes can prevent an increase in the nonspecific detection level caused by cross-reactions. Therefore, changes in IGLV1-40 and IGHV4-4 plasma exosomes exhibit significant potential for NSCLC diagnosis.

ROC curve analysis is a commonly used statistical method during clinical diagnostic tests [40, 41]. The AUC value can be used to evaluate the diagnostic ability of test indexes directly. To clarify the diagnostic value of IGLV1-40 and IGHV4-4, the NSCLC samples were further expanded to 71 cases and the HC samples to 40 cases. The AUC values of these two subtypes were counted using the ROC curve technique. Compared with the non-metastatic group, the IGHV4-4 AUC was 0.71 in the metastatic group while presenting values of 0.83 in the NSCLC group and 0.80 in the non-metastatic group compared with the HCs. Moreover, IGLV1-40 alone displayed a more significant AUC value for LC diagnosis. The AUC values were 0.88 and 0.85, respectively, after comparing the NSCLC and non-metastatic groups with the HC group and 0.74 when comparing the metastatic and non-metastatic groups. However, the diagnostic values of these two molecules alone fail to meet the requirements for clinical LC diagnosis. This study also evaluated the combined diagnosis values of IGLV1-40 and IGHV4-4. The AUC values of the NSCLC

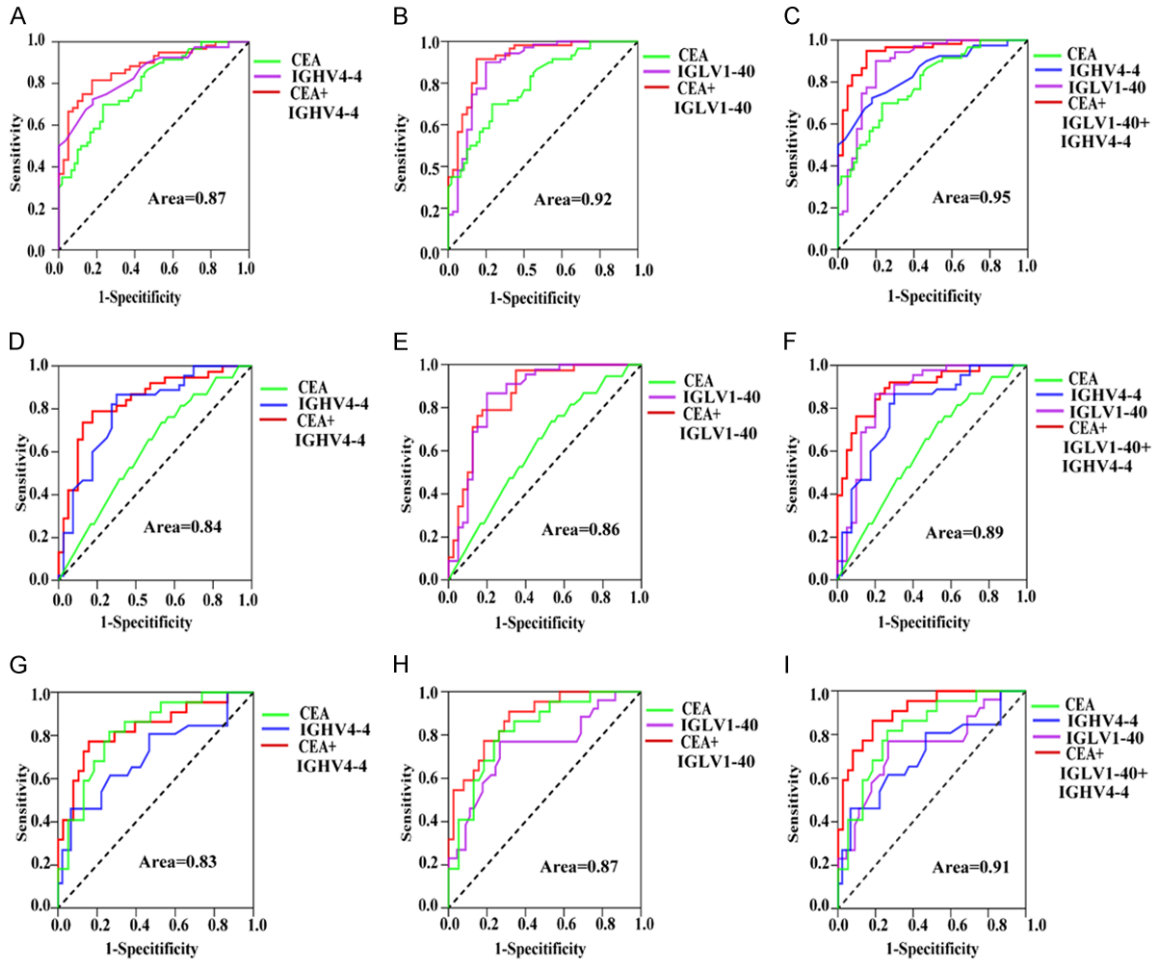

Figure 7. The ROC curve analysis of the combined exosomal IGLV1-40, IGHV4-4, and serum CEA of the NSCLC patients. (A-C) The ROC curves to distinguish between the NSCLC patients (n=84) and the HCs (n=84). The ROC curves of the combined IGHV4-4 and CEA (A), combined IGLV1-40 and CEA (B), and combined IGHV4-4, IGLV1-40, and CEA (C). (D-F) The ROC curves distinguishing between the non-metastatic patients (n=45) and HCs. The ROC curves of the combined IGHV4-4 and CEA (D), combined IGLV1-40 and CEA (E), and combined IGHV4-4, IGLV1-40, and CEA (F). (G-I) The ROC curves to distinguish between non-metastatic and metastatic patients (n=39). The ROC curves of the combined IGHV4-4 and CEA (G), combined IGLV1-40 and CEA (H), and combined IGHV4-4, IGLV1-40, and CEA (I).

and non-metastatic groups were 0.93 and 0.89, respectively, and 0.83 when comparing the metastatic and non-metastatic groups, suggesting that combining IGLV1-40 and IGHV4-4 can significantly improve the ability to diagnose LC.

Although CEA is a commonly used biomarker for LC diagnosis, its sensitivity and specificity are unsatisfactory, and its clinical applicability is limited. Therefore, it is not generally recommended as a tool for early LC detection [42]. This study indicated that the diagnostic values when combining IGLV1-40 and IGHV4-4 with CEA was significantly higher than CEA alone and could distinguish metastatic from non-metastatic cancer. In particular, the IGLV1-40 and CEA combination presented higher diagnostic values. The AUC values were 0.92 (90.00% sensitivity and 85.00% specificity) and 0.86 (73.68% sensitivity and 85.00% specificity), respectively, in NSCLC and non-metastatic cancer, compared with the HCs. Compared with the non-metastatic group, the AUC value in the metastatic group was 0.87 (54.55% sensitivity and 92.11% specificity). Moreover, when combined with CEA, the diagnostic ability of IGLV1-40 and IGHV4-4 significantly exceeded their individual performance. Compared with the HCs, the NSCLC and non-metastatic groups displayed AUCs of 0.95 (95.00% sensitivity and 85.00% specificity)

and 0.89 (76.32% sensitivity and 82.50% specificity), respectively, and 0.91 (72.73% sensitivity and 89.47% specificity) when comparing the non-metastatic and metastatic groups. These results indicated that IGLV1-40 and IGHV4-4 enhanced CEA diagnostic efficacy.

This study indicates that the plasma exosomes display a large number of LC-labeled immunoglobulin subtypes, presenting new ways for using exosome immunoglobulin subtypes for LC liquid biopsy. The immunoglobulin subtype diversity represents the core of the immune response theory. Its role in disease occurrence has attracted increasing attention. However, some questions remain: (1) whether the immunoglobulin subtype changes are related to the progression of LC and clinical parameters, (2) whether the immunoglobulin subtype content in patients with NSCLC coincides with clinical symptoms, and (3) whether the changes in the immunoglobulin subtypes derived from B cells in patients with LC are similar to those in serum. Further examination of the expression characteristics of these immunoglobulin subtypes in blood or B cells may enhance the understanding of the immunopathological mechanism of LC, as well as diagnosing and treating this disease.

Acknowledgements

This study was supported by the Science and Technology Foundation of Guizhou (5766-07), the Science and Technology Planning Foundation of Guiyang ([2019]-9-4-37), and the Scientific Research Project of the Second Affiliated Hospital of Guizhou University of Traditional Chinese Medicine (GZEYK[2020]26).

Disclosure of conflict of interest

None.

Address correspondence to: Jie Gong and Hongping Ba, Department of Clinical Laboratory, Wuhan Center for Clinical Laboratory, Wuhan 430015, Hubei, PR China. Tel: +86-027-85698607; E-mail: gongjie@whccl.org (JG); Tel: +86-027-856-98605; E-mail: bhpsky@163.com (HPB)

References

[1] Torre LA, Bray F, Siegel RL, Ferlay J, Lortet-Tieulent J and Jemal A. Global cancer statistics, 2012. CA Cancer J Clin 2015; 65: 87-108.

[2] Edwards BK, Brown ML, Wingo PA, Howe HL, Ward E, Ries LA, Schrag D, Jamison PM, Jemal A, Wu XC, Friedman C, Harlan L, Warren J, Anderson RN and Pickle LW. Annual report to the nation on the status of cancer, 1975-2002, featuring population-based trends in cancer treatment. J Natl Cancer Inst 2005; 97: 1407-1427.

[3] Ezer N, Navasakulpong A, Schwartzman K, Ofiara L and Gonzalez AV. Impact of rapid investigation clinic on timeliness of lung cancer diagnosis and treatment. BMC Pulm Med 2017; 17: 178.

[4] Li W, Li C, Zhou T, Liu X, Liu X, Li X and Chen D. Role of exosomal proteins in cancer diagnosis. Mol Cancer 2017; 16: 145.

[5] Gowda R, Robertson BM, Iyer S, Barry J, Dinavahi SS and Robertson GP. The role of exosomes in metastasis and progression of melanoma. Cancer Treat Rev 2020; 85: 101975.

[6] Whitehead B, Wu L, Hvam ML, Aslan H, Dong M, Dyrskjot L, Ostenfeld MS, Moghimi SM and Howard KA. Tumour exosomes display differential mechanical and complement activation properties dependent on malignant state: implications in endothelial leakiness. J Extracell Vesicles 2015; 4: 29685.

[7] Li S, Yi M, Dong B, Tan X, Luo S and Wu K. The role of exosomes in liquid biopsy for cancer diagnosis and prognosis prediction. Int J Cancer 2021; 148: 2640-2651.

[8] Zhou B, Xu K, Zheng X, Chen T, Wang J, Song Y, Shao Y and Zheng S. Application of exosomes as liquid biopsy in clinical diagnosis. Signal Transduct Target Ther 2020; 5: 144.

[9] Watson CT, Glanville J and Marasco WA. The individual and population genetics of antibody immunity. Trends Immunol 2017; 38: 459-470.

[10] Zuo T, Gautam A and Wesemann DR. Affinity war: forging immunoglobulin repertoires. Curr Opin Immunol 2019; 57: 32-39.

[11] Berget E, Molven A, Lokeland T, Helgeland L and Vintermyr OK. IGHV gene usage and mutational status in follicular lymphoma: correlations with prognosis and patient age. Leuk Res 2015; 39: 702-708.

[12] Pascual V, Victor K, Lelsz D, Spellerberg MB, Hamblin TJ, Thompson KM, Randen I, Natvig J, Capra JD and Stevenson FK. Nucleotide sequence analysis of the V regions of two IgM cold agglutinins. Evidence that the VH4-21 gene segment is responsible for the major cross-reactive idiotype. J Immunol 1991; 146: 4385-4391.

[13] Schickel JN, Glauzy S, Ng YS, Chamberlain N, Massad C, Isnardi I, Katz N, Uzel G, Holland SM, Picard C, Puel A, Casanova JL and Meffre E. Self-reactive VH4-34-expressing IgG B cells

recognize commensal bacteria. J Exp Med 2017; 214: 1991-2003.
[14] Tipton CM, Fucile CF, Darce J, Chida A, Ichikawa T, Gregoretti I, Schieferl S, Hom J, Jenks S, Feldman RJ, Mehr R, Wei C, Lee FE, Cheung WC, Rosenberg AF and Sanz I. Diversity, cellular origin and autoreactivity of antibody-secreting cell population expansions in acute systemic lupus erythematosus. Nat Immunol 2015; 16: 755-765.
[15] Goldstraw P, Chansky K, Crowley J, Rami-Porta R, Asamura H, Eberhardt WE, Nicholson AG, Groome P, Mitchell A and Bolejack V; International Association for the Study of Lung Cancer Staging and Prognostic Factors Committee, Advisory Boards, and Participating Institutions; International Association for the Study of Lung Cancer Staging and Prognostic Factors Committee Advisory Boards and Participating Institutions. The IASLC lung cancer staging project: proposals for revision of the TNM stage groupings in the forthcoming (Eighth) edition of the TNM classification for lung cancer. J Thorac Oncol 2016; 11: 39-51.
[16] Lobb RJ, Becker M, Wen SW, Wong CS, Wiegmans AP, Leimgruber A and Moller A. Optimized exosome isolation protocol for cell culture supernatant and human plasma. J Extracell Vesicles 2015; 4: 27031.
[17] Qi Z, Xue Q, Wang H, Cao B, Su Y, Xing Q and Yang JJ. Serum CD203c+ extracellular vesicle serves as a novel diagnostic and prognostic biomarker for succinylated gelatin induced perioperative hypersensitive reaction. Front Immunol 2021; 12: 732209.
[18] Thery C, Amigorena S, Raposo G and Clayton A. Isolation and characterization of exosomes from cell culture supernatants and biological fluids. Curr Protoc Cell Biol 2006; Chapter 3: Unit 3.22.
[19] Ogese MO, Jenkins RE, Adair K, Tailor A, Meng X, Faulkner L, Enyindah BO, Schofield A, Diaz-Nieto R, Ressel L, Eagle GL, Kitteringham NR, Goldring CE, Park BK, Naisbitt DJ and Betts C. Exosomal transport of hepatocyte-derived drug-modified proteins to the immune system. Hepatology 2019; 70: 1732-1749.
[20] Capello M, Vykoukal JV, Katayama H, Bantis LE, Wang H, Kundnani DL, Aguilar-Bonavides C, Aguilar M, Tripathi SC, Dhillon DS, Momin AA, Peters H, Katz MH, Alvarez H, Bernard V, Ferri-Borgogno S, Brand R, Adler DG, Firpo MA, Mulvihill SJ, Molldrem JJ, Feng Z, Taguchi A, Maitra A and Hanash SM. Exosomes harbor B cell targets in pancreatic adenocarcinoma and exert decoy function against complement-mediated cytotoxicity. Nat Commun 2019; 10: 254.
[21] Baassiri A, Nassar F, Mukherji D, Shamseddine A, Nasr R and Temraz S. Exosomal non coding RNA in LIQUID biopsies as a promising biomarker for colorectal cancer. Int J Mol Sci 2020; 21: 1398.
[22] Bashford-Rogers RJM, Smith KGC and Thomas DC. Antibody repertoire analysis in polygenic autoimmune diseases. Immunology 2018; 155: 3-17.
[23] Cao J, Zhang M, Xie F, Lou J, Zhou X, Zhang L, Fang M and Zhou F. Exosomes in head and neck cancer: roles, mechanisms and applications. Cancer Lett 2020; 494: 7-16.
[24] Halvaei S, Daryani S, Eslami SZ, Samadi T, Jafarbeik-Iravani N, Bakhshayesh TO, Majidzadeh AK and Esmaeili R. Exosomes in cancer liquid biopsy: a focus on breast cancer. Mol Ther Nucleic Acids 2018; 10: 131-141.
[25] Rolfo C, Castiglia M, Hong D, Alessandro R, Mertens I, Baggerman G, Zwaenepoel K, Gil-Bazo I, Passiglia F, Carreca AP, Taverna S, Vento R, Santini D, Peeters M, Russo A and Pauwels P. Liquid biopsies in lung cancer: the new ambrosia of researchers. Biochim Biophys Acta 2014; 1846: 539-546.
[26] Borghaei H, Paz-Ares L, Horn L, Spigel DR, Steins M, Ready NE, Chow LQ, Vokes EE, Felip E, Holgado E, Barlesi F, Kohlhäufl M, Arrieta O, Burgio MA, Fayette J, Lena H, Poddubskaya E, Gerber DE, Gettinger SN, Rudin CM, Rizvi N, Crinò L, Blumenschein GR Jr, Antonia SJ, Dorange C, Harbison CT, Graf Finckenstein F and Brahmer JR. Nivolumab versus docetaxel in advanced nonsquamous non-small-cell lung cancer. N Engl J Med 2015; 373: 1627-1639.
[27] Hemperly A and Vande Casteele N. Clinical pharmacokinetics and pharmacodynamics of infliximab in the treatment of inflammatory bowel disease. Clin Pharmacokinet 2018; 57: 929-942.
[28] Jorgensen KK, Olsen IC, Goll GL, Lorentzen M, Bolstad N, Haavardsholm EA, Lundin KEA, Mork C, Jahnsen J and Kvien TK; NOR-SWITCH study group. Switching from originator infliximab to biosimilar CT-P13 compared with maintained treatment with originator infliximab (NOR-SWITCH): a 52-week, randomised, double-blind, non-inferiority trial. Lancet 2017; 389: 2304-2316.
[29] Shanafelt TD, Wang XV, Kay NE, Hanson CA, O'Brien S, Barrientos J, Jelinek DF, Braggio E, Leis JF, Zhang CC, Coutre SE, Barr PM, Cashen AF, Mato AR, Singh AK, Mullane MP, Little RF, Erba H, Stone RM, Litzow M and Tallman M. Ibrutinib-rituximab or chemoimmunotherapy for chronic lymphocytic leukemia. N Engl J Med 2019; 381: 432-443.
[30] Tausch E, Schneider C, Robrecht S, Zhang C, Dolnik A, Bloehdorn J, Bahlo J, Al-Sawaf O, Rit-

gen M, Fink AM, Eichhorst B, Kreuzer KA, Tandon M, Humphrey K, Jiang Y, Schary W, Bullinger L, Mertens D, Lurà MP, Kneba M, Döhner H, Fischer K, Hallek M and Stilgenbauer S. Prognostic and predictive impact of genetic markers in patients with CLL treated with obinutuzumab and venetoclax. Blood 2020; 135: 2402-2412.

[31] Bashford-Rogers RJM, Bergamaschi L, McKinney EF, Pombal DC, Mescia F, Lee JC, Thomas DC, Flint SM, Kellam P, Jayne DRW, Lyons PA and Smith KGC. Analysis of the B cell receptor repertoire in six immune-mediated diseases. Nature 2019; 574: 122-126.

[32] Gaillard AW. Effects of warning-signal modality on the contingent negative variation (CNV). Biol Psychol 1976; 4: 139-154.

[33] Huang DF, Siminovitch KA, Liu XY, Olee T, Olsen NJ, Berry C, Carson DA and Chen PP. Population and family studies of three disease-related polymorphic genes in systemic lupus erythematosus. J Clin Invest 1995; 95: 1766-1772.

[34] Mo L, Leu SJ, Berry C, Liu F, Olee T, Yang YY, Beardsley DS, McMillan R, Woods VL Jr and Chen PP. The frequency of homozygous deletion of a developmentally regulated Vh gene (Humhv3005) is increased in patients with chronic idiopathic thrombocytopenic purpura. Autoimmunity 1996; 24: 257-263.

[35] Tsai FJ, Lee YC, Chang JS, Huang LM, Huang FY, Chiu NC, Chen MR, Chi H, Lee YJ, Chang LC, Liu YM, Wang HH, Chen CH, Chen YT and Wu JY. Identification of novel susceptibility Loci for Kawasaki disease in a Han Chinese population by a genome-wide association study. PLoS One 2011; 6: e16853.

[36] Sawcer S, Jones HB, Feakes R, Gray J, Smaldon N, Chataway J, Robertson N, Clayton D, Goodfellow PN and Compston A. A genome screen in multiple sclerosis reveals susceptibility loci on chromosome 6p21 and 17q22. Nat Genet 1996; 13: 464-468.

[37] Walter MA, Gibson WT, Ebers GC and Cox DW. Susceptibility to multiple sclerosis is associated with the proximal immunoglobulin heavy chain variable region. J Clin Invest 1991; 87: 1266-1273.

[38] Guo C, Gao YY, Ju QQ, Zhang CX, Gong M and Li ZL. HELQ and EGR3 expression correlate with IGHV mutation status and prognosis in chronic lymphocytic leukemia. J Transl Med 2021; 19: 42.

[39] Shi K, Sun Q, Qiao C, Zhu H, Wang L, Wu J, Wang L, Fu J, Young KH, Fan L, Xia Y, Xu W and Li J. 98% IGHV gene identity is the optimal cut-off to dichotomize the prognosis of Chinese patients with chronic lymphocytic leukemia. Cancer Med 2020; 9: 999-1007.

[40] Mandrekar JN. Receiver operating characteristic curve in diagnostic test assessment. J Thorac Oncol 2010; 5: 1315-1316.

[41] Obuchowski NA and Bullen JA. Receiver operating characteristic (ROC) curves: review of methods with applications in diagnostic medicine. Phys Med Biol 2018; 63: 07TR01.

[42] Okamura K, Takayama K, Izumi M, Harada T, Furuyama K and Nakanishi Y. Diagnostic value of CEA and CYFRA 21-1 tumor markers in primary lung cancer. Lung Cancer 2013; 80: 45-49.

Supplementary Table 1. GO cellular component enrichment analysis of DEPs from the exosomes of NSCLC patients and HCs (The top 5 terms)

GO ID	GO term	Number of enrichment	*P* value	Enrichment
GO:0019814	Immunoglobulin complex	18	0.004584	2.338783
GO:0005886	Plasma membrane	26	0.026586	1.575354
GO:0042571	immunoglobulin complex circulating	12	0.032084	1.493708
GO:0071752	secretory dimeric IgA immunoglobulin complex	2	0.068014	1.167402
GO:0009897	external side of plasma membrane	12	0.106242	0.973705

Supplementary Table 2. GO molecular function enrichment analysis of DEPs from the exosomes of NSCLC patients and HCs (The top 5)

GO ID	GO term	Number of enrichment	Enrichment	*P* Value
GO:0003823	antigen binding	22	2.72713	0.001874
GO:0034987	immunoglobulin receptor binding	12	1.51937	0.030243
GO:0071723	lipopeptide binding	1	0.774221	0.168182
GO:0070891	Lipoteichoic acid binding	1	0.774221	0.168182
GO:0008431	vitamin E binding	1	0.774221	0.168182

Supplementary Table 3. ROC analysis of the exosomal IGHV4-4 and IGLV1-40 protein

Protein name	Comparison between the NSCLC and HCs			Comparison between the non-metastatic patients and HCs			Comparison between the metastatic and on-metastatic patients		
	AUC	Sensitivity	Specificity	AUC	Sensitivity	Specificity	AUC	Sensitivity	Specificity
IGLV1-40	0.88	90.14%	80.00%	0.85	86.67%	80.14%	0.74	76.87%	73.13%
IGHV4-4	0.83	85.92%	70.00%	0.80	83.71%	70.33%	0.71	46.22%	93.31%
IGLV1-40+IGHV4-4	0.93	88.73%	85.00%	0.89	86.05%	81.03%	0.83	83.34%	77.81%

Supplementary Table 4. Diagnostic value of exosomal immunoglobulins with CEA biomarker

Gene symbol	Comparison between the NSCLC and HCs			Comparison between the non-metastatic patients and HCs			Comparison between the metastatic and on-metastatic patients		
	AUC	Sensitivity	Specificity	AUC	Sensitivity	Specificity	AUC	Sensitivity	Specificity
CEA	0.78	70.00%	76.67%	0.61	51.32%	60.15%	0.81	80.60%	77.80%
CEA+IGHV4-4	0.87	81.67%	77.50%	0.84	78.95%	82.50%	0.83	72.73%	86.84%
CEA+IGLV1-40	0.92	85.00%	90.00%	0.86	73.68%	85.00%	0.87	54.55%	92.11%
CEA+IGHV4-4+IGLV1-40	0.95	90.00%	85.00%	0.89	76.32%	82.50%	0.91	72.73%	89.47%